HHS Public Access

Author manuscript

ACS Appl Mater Interfaces. Author manuscript; available in PMC 2023 April 20.

Published in final edited form as:

ACS Appl Mater Interfaces. 2022 April 20; 14(15): 17940–17949. doi:10.1021/acsami.1c25218.

Slippery Anti-Fouling Polymer Coatings Fabricated Entirely from Biodegradable and Biocompatible Components

Harshit Agarwal[1], **La'Darious J. Quinn**[2], **Sahana C. Walter**[1], **Thomas J. Polaske**[2], **Douglas H. Chang**[1], **Sean P. Palecek**[1], **Helen E. Blackwell**[2], **David M. Lynn**[1,2]

[1]Dept. of Chemical and Biological Engineering, Univ. of Wisconsin–Madison, 1415 Engineering Dr., Madison, WI 53706

[2]Dept. of Chemistry, Univ. of Wisconsin–Madison, 1101 University Ave., Madison, WI 53706, USA

Abstract

We report on the design of slippery liquid-infused porous surfaces (SLIPS) fabricated entirely from building blocks that are biodegradable, edible, or generally regarded to be biocompatible. Our approach involves infusion of lubricating oils, including food oils, into nanofiber-based mats fabricated by electrospinning or blow spinning of poly(ε-caprolactone), a hydrophobic biodegradable polymer used widely in medical implants and drug delivery devices. This approach leads to durable and biodegradable SLIPS that prevent fouling by liquids and other materials, including microbial pathogens, on objects of arbitrary shape, size, and topography. This degradable polymer approach also provides practical means to design 'controlled release' SLIPS that release molecular cargo at rates that can be manipulated by the properties of the infused oils (e.g., viscosity or chemical structure). Together, our results provide new designs and introduce useful properties and behaviors to anti-fouling SLIPS, address important issues related to biocompatibility and environmental persistence, and thus advance new potential applications, including the use of slippery materials for food packaging, industrial and marine coatings, and biomedical implants.

Graphical Abstract

(D.M.L.) dlynn@engr.wisc.edu.

Supporting Information. Descriptions of materials and methods and additional microscopy images, plots, and videos used for characterizion of the structures and behaviors of slippery surfaces (PDF). This material is available free of charge via the Internet.

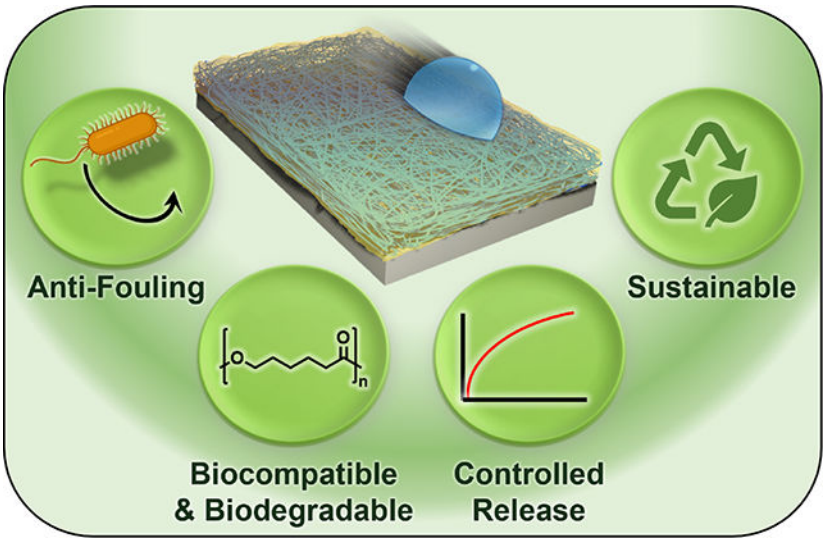

Keywords

Slippery; Antifouling; Liquid-Infused; Controlled Release; Polymers

Introduction

The accumulation of unwanted substances or organisms on surfaces is a widespread problem in industrial, healthcare, and consumer settings, and can lead to costly economic burdens or, in biomedical and clinical contexts, to pain, suffering, and loss of life.[1,2] Surfaces and coatings that can reduce or prevent fouling in complex aqueous, marine, or biological environments thus have enormous practical utility. Many strategies have been used to design such materials, most of which are based on chemical functionalization, structural modification of the substrate, or some combination of both.[3–9] However, despite decades of research and development, several important issues associated with the design, production, and application of anti-fouling materials remain unaddressed, including concerns related to functional failure in complex environments and the use of building blocks and design approaches that pose environmental concerns. For example, many current designs for single-use packaging often lead to considerable product wastage (e.g., resulting from the sticking or inefficient drainage of liquid foods or other commercial fluids), and many “non-stick” flexible packaging materials are not recyclable and contain environmentally harmful components [e.g., perfluoroalkyl and polyfluoroalkyl substances (PFAS)]. In general, the design of physically and chemically robust anti-fouling surfaces that are simple, scalable, and sustainable remains a significant challenge.

This current study was motivated broadly by recent advances toward the design and application of so-called ‘slippery liquid infused porous surfaces’ (SLIPS) or ‘lubricant impregnated surfaces’ (LIS).[10–16] These materials represent an emerging class of bio-inspired synthetic surface coatings that exhibit unique anti-fouling properties.[13–16] They are typically fabricated by the infusion of a lubricating hydrophobic oil into a porous or textured solid matrix, yielding surfaces with smooth and mobile interfaces that permit

immiscible liquids and other materials to simply slide off. In addition to strong anti-fouling properties, these materials also offer platforms for fabricating complex and responsive interfaces by manipulating the functional properties of either the infused liquid or the underlying porous matrix.[16–18] As a result, these materials have potential utility in many potential applications, including to prevent biofouling,[13,19–25] reduce drag,[26,27] impart anti-icing properties,[28,29] and manipulate the behaviors of droplets on surfaces.[16–18] Over the last decade, major advances have been made related to the manufacturing, versatility, and durability of SLIPS-based materials, and several leading designs have been commercialized to reduce surface fouling in consumer and marine environments. The growing importance and rapid commercial adoption of these anti-fouling materials raise questions about potential environmental impacts that could be associated with the fabrication, utilization, and persistence of liquid-infused surfaces and, in general, the sustainable design of SLIPS and LIS remains a challenge.

In this paper, we report strategies for the design of polymer-based SLIPS that are readily biodegradable and can be constructed entirely from common and readily available building blocks that are degradable, edible, or generally regarded to be biocompatible. These strategies are based on the infusion of lubricating oils, including food oils, into porous nanofiber-based networks that are produced by the electrospinning or blow spinning of poly(ε-caprolactone) (PCL), a hydrophobic polyester used widely in biomedical applications. These degradable SLIPS can resist or prevent fouling by a range of liquids, materials, and microorganisms, including common fungal and bacterial pathogens. The approaches reported here also provide opportunities to incorporate controlled release behaviors; we demonstrate, for example, that molecular cargo can be released from these anti-fouling coatings at rates that can be manipulated by the properties (e.g., viscosity or chemical structure) of the infused oils. Overall, these fabrication approaches are straightforward to implement, scalable, and can be used to generate slippery coatings on surfaces of arbitrary size and shape. Our results expand the range of properties and behaviors that can be designed into SLIPS and take an important step toward addressing issues related to their sustainability and environmental impacts and, thereby, advance toward potential new applications including, the use of slippery materials for food packaging, industrial and marine coatings, and biomedical implants.

Materials and Methods

Materials.

Dichloromethane (DCM), *N,N*-dimethylformamide (DMF), calcium chloride (anhydrous, ≥ 97%), poly(ε-caprolactone) (PCL, M_n = 80,000), sodium citrate tribasic dihydrate (≥ 99.0%), sodium chloride (NaCl, ≥ 99.0%), menadione, melittin (from honeybee venom, ≥ 85%), glycerol (≥ 99.0%), and silicone oil (for oil baths [υ ~ 50 cSt and υ = 500 cSt]) were obtained from Millipore Sigma (Milwaukee, WI). Tris-HCL and Triton X-100 were obtained from Promega (Madison, WI). 3-(*N*-morpholino)propanesulfonic acid (MOPS) and tetrahydrofuran (THF) were obtained from Fisher Scientific (Pittsburgh, PA). Methanol (≥99.9%) was obtained from VWR International. Ethanol (200 proof) was purchased from Decon Laboratories (King of Prussia, PA). 5-(and-6)-carboxytetramethyl rhodamine (TMR)

was purchased from Setareh Biotech (Eugene, OR). Glurataldehyde (50% solution) was purchased from Electron Microscopy Sciences (Washington, PA). Samples of lake water, beer, tomato ketchup, soy sauce, and pooled human urine were obtained as described previously.[30] Rust Oleum commercial 5200 system (DTM acrylic) was purchased from The Home Depot (Madison, WI). Fresh porcine blood was collected, stored, and prepared as described previously.[31] Phosphate-buffered saline (PBS) was prepared from concentrate (Millipore-Sigma, Milwaukee, WI). Brain heart infusion (BHI) medium was obtained from Teknova (Hollister, CA). Lennox L Broth (LB) medium was obtained from Research Products International (Mt. Prospect, IL). Gibco brand RPMI 1640 powder (containing phenol red and L-glutamine and without sodium bicarbonate or HEPES), Dulbecco's modified Eagle's medium (DMEM), Dulbecco's phosphate-buffered saline (DPBS, without calcium or magnesium), and trypsin-EDTA (0.25%, with phenol red), SYTO-9 stain, and FUN-1 stain were obtained from ThermoFisher Scientific (Waltham, MA). Freshly expired human red blood cells (hRBCs) were obtained as described previously.[30] Fetal bovine serum (FBS) was obtained from Peak Serum (Wellington, CO). Water (18.2 MΩ) was purified using a Millipore filtration system. All materials were used as received without additional purification unless noted otherwise.

General Considerations.

Scanning electron micrographs were prepared and acquired using general procedures described previously.[31,32] For cross-sectional images, samples were scored and dipped in liquid N_2 for two minutes. After the substrates were completely frozen, they were quickly removed from the liquid N_2 and manually snapped along the scored line. Pictures and videos were recorded on a smartphone (Samsung Galaxy S8+). Contact angle measurements were recorded as described previously.[32] using both the droplet volume change and tilting methods (see the Results and Discussion section for more details). Solution fluorescence was measured using an EL800 Universal Microplate Reader (Bio-Tek Instruments). ImageJ software (version 1.51j8) was used to characterize fiber diameters. Fluorescence microscopy images were acquired and analyzed as described previously.[32] Numerical data were processed using Microsoft Excel and plotted using GraphPad Prism 7 (version 7.0h). Compressed air was filtered through a membrane syringe filter (0.2 μm).

Electrospinning of Nanofiber-Based Coatings.

A 150 mg/mL polymer solution was made by dissolving PCL into a 1:1 mixture of DMF and THF. For fabrication of TMR-loaded nanofiber-based coatings, ~0.5 mg/mL of TMR was added into the polymer solutions before electrospinning. Fibers were produced using an electrospinning device with a digital syringe pump and a flow rate of 1.5 mL/h (225 mg/hr). The blunt 22G needle and the grounded collector were separated by a working distance of 30 cm, as described previously,[33] and a 20 kV potential (or 25 kV for the TMR-loaded fibers) was applied between the collector and the needle tip. Fibers were accumulated for ~5 min on substrates (e.g., aluminum foil, glass slides, and flexible polyester films) placed directly on the ground collector (e.g., see schematic and discussion below). All nanofiber coatings were kept in vacuum desiccators prior to use.

Fabrication of Nanofiber Coatings by Blow Spinning.

PCL solution (5% w/v in DCM) was loaded into a 6 mL syringe. The co-axial syringe (AliExpress) was positioned in a syringe pump and then connected to the inner (22G) nozzle. The outer (17G) nozzle was connected to a compressed nitrogen tank. Before spraying, the substrate was placed in a position located ~7.5 cm away the tip of the nozzle. The pump delivered at a rate 2.4 mL/hr (120 mg/hr) and the gas pressure supplied was 20 psi (0.138 MPa). Each substrate was sprayed with PCL until a uniform coating was obtained (~2 minutes for a 2 cm^2 substrate). The total spraying time varied depending on the substrate. For TMR-loaded PCL fibers, ~0.5 mg/mL TMR was dissolved in a 5 wt% PCL solution in (8:1) v/v DCM:MeOH. The solution was then thoroughly vortexed and sonicated to ensure complete mixing before loading into a syringe. The rest of the fabrication parameters and methods were kept constant to those for the blow spinning of unloaded PCL.

Preparation of Slippery Surfaces and Measurement of Sliding Times.

Coatings produced by electrospinning and blow spinning were infused with oils in the following general manner. Oil droplets (~10 μL) were placed at different spots onto a coated surface tilted at angles ranging from 70° to 90°. The samples were left tilted for ~30 min before use to permit oil to spread and to allow excess lubricant to drain off the substrates through gravity-driven processes. Measurements of the sliding times for droplets of test fluids (20 μL; see Results and Discussion section for additional details) were made as previously described.[32]

Loading and Release of TMR.

TMR-loaded nanofiber-mats coated onto glass slides (1 × 2.0 cm; 2 cm^2) were infused with different lubricating liquids (see Results and Discussion section for additional details) using the procedure described above. All of the infused and non-infused substrates (n=4) were incubated at 37 °C or 4 °C in 4 mL of PBS at pH 7.4. At predetermined times, buffer was analyzed using a fluorometer and replaced with new buffer. To characterize the total amount of TMR incorporated into these nanofiber-mats, TMR was extracted from the mats by stirring (at 200 rpm) TMR-loaded mats (1 × 1.0 cm; 1 cm^2) in 500 μL DMF at room temperature for 30 min, followed by sonication for 5 s. The samples were then centrifuged at 5000g for 1 min to separate out any polymer particulates. The DMF solution was isolated and diluted 9× in water, and TMR extracted from the mats into DMF was measured using a fluorometer and compared to a standard curve of TMR in Milli-Q water:DMF [1:9]).

Characterization of Fungal Biofilm on SLIPS-Coated Surfaces.

Candida albicans (SC 5314) was purchased from ATCC (Manassas, VA) and was streaked on a yeast peptone dextrose (YPD) agar plate from a frozen stock solution and grown overnight at 30 °C. For each assay, a colony was collected from the YPD plate and grown overnight in 15 mL centrifuge tubes at 30 °C in liquid YPD broth, and cells were then washed, resuspended, and prepared for subsequent experiments as described previously.[25] PCL nanofiber meshes were cut into multiple 1 × 1 cm segments. Each segment was individually stuck to the bottom of a well in a 24-well microtiter plate, and then infused with silicone oil. Bare uncoated wells were used as controls. *C. albicans* subculture (1 mL) was

added to each well and incubated at 37 °C without shaking. After 24 h, the wells were rinsed two times with PBS to remove planktonic cells and loosely bound biofilms and then stained using a green fluorescent stain (FUN-1). Excess stain was dabbed with a paper towel and substrates were then placed into new wells and characterized by fluorescence microscopy.

Characterization of Bacterial Biofilm on SLIPS-Coated Surfaces.

Freezer stocks of (i) *Staphylococcus aureus* (RN6390b)[34] in BHI medium:glycerol (1:1; 50% (v/v) in water) and (ii) *Escherichia coli* (K-12 MG1655; obtained from The Coli Genetic Stock Center, Yale University) in 1:1 LB medium:glycerol (50% (v/v) in water) were maintained at −80 °C. Overnight cultures were grown at 37 °C in LB medium or BHI medium with shaking at 200 rpm. The overnight cultures were then resuspended (1:100) in fresh BHI (+ 1% (w/v) glucose) or fresh LB medium. SLIPS-coated substrates and bare glass plates were positioned in the wells of a 24-well plate. Bacterial subculture (1 mL) was then added and incubated at 37 °C under static conditions. After 24 h, samples were washed 2x with DI water and stained with SYTO-9. Excess stain was dabbed with a paper towel and substrates were then placed into new wells and characterized by fluorescence microscopy.

Characterization of Mammalian Cells Adhesion.

Bare glass and SLIPS-coated surfaces were sterilized using UV light for 20 min prior to use and placed in a 24-well tissue culture-treated polystyrene microtiter plate. 3T3 mouse fibroblast (NIH/3T3) cells were grown in 6-well plates at 37 °C and 5% CO_2 in DMEM containing 10% v/v fetal bovine serum, 100 μg/mL streptomycin, and 100 units/mL penicillin. Cells were passaged upon 70–80% confluency by gently washing the cell layer with PBS and then detaching them from the bottom of the wells with a 0.25% trypsin-EDTA solution. Confluent 3T3 cells from an ongoing cell line were detached during passaging and seeded onto experimental surfaces at initial densities of 100,000 cells/mL in 750 μL of medium and then maintained at 37 °C for 24 h. Following incubation, growth medium was aspirated and samples were rinsed washed twice gently using PBS. For imaging, cells were stained using SYTO-9 for 30 min. The staining solution was then removed and substrates were transferred to new wells and imaged by fluorescence microscopy.

Hemolysis Assays.

Hemolysis assays were performed based on previously reported protocols with some minor modifications.[30,35,36] Aliquots (400 μL) of hRBCs in TBS were pipetted on top of SLIPS-coated and uncoated glass slides (1 × 1 cm) stored in the wells of a 24-well plate and the samples were incubated at 37 °C for three hours. Samples were then treated, processed, measured, and analyzed as reported previously.[30]

Platelet Adhesion Assays.

Platelet adhesion assays were performed using methods reported previously with some minor modifications.[30] Uncoated glass samples and SLIPS-coated samples were positioned in 24-well plates, platelet solution (700 μL) was added to each well, and samples were incubated statically at 37 °C for 2 hours. Platelet solution was then removed and samples

were then washed with water and fixed using a 2.5 wt% solution of glutaraldehyde for 10 h at 4 °C. The samples were then dehydrated, sputtered with gold, and characterized by SEM.

Other Characterization of Liquid-Infused Surfaces.

To characterize stability and slippery behavior upon immersion in ketchup, a SLIPS-coated glove was immersed in a beaker full of ketchup 10×, with each dipping cycle lasting for few seconds. The influence of smudging was characterized by touching and rubbing liquid-infused materials with a gloved finger using moderate pressure ~10 times in different areas of the coated substrate. To characterize stability to rubbing and abrasion, a laboratory Kimwipe was rubbed along the coated surface of polycarbonate laboratory glasses with moderate pressure for ~1 minute. The stability of liquid-infused materials upon exposure to blood was evaluated by repeated (~10×) dispensing of blood on a SLIPS-coated watch glass and then tilting the substrate to remove the blood.

Results and Discussion

The strategy reported here for the design of biocompatible and biodegradable SLIPS is based on infusion of slippery lubricating liquids, or oils, into nanofiber-based meshes fabricated by the electrospinning or blow spinning of PCL. This approach is illustrated schematically in Figure 1A. We focused on this approach for several reasons: (i) electrospinning and blow spinning are both well-developed technologies that can be used to create polymer matrices (or ‘mats’) with interconnected, 3-D porous structures and high internal surface areas that can accept, contain, and host liquid phases,[37–40] (ii) PCL is a readily-available biocompatible and biodegradable polyester that is used extensively in surgical implants and drug delivery devices,[41] and (iii) PCL is hydrophobic, exhibits good water resistance, and degrades very slowly in many aqueous environments,[41] providing a matrix that we hypothesized would be useful for the infusion and stable retention of hydrophobic oils without the need for additional chemical functionalization or the synthesis of new chemically compatible building blocks. Our results reveal that PCL mats can be infused to generate SLIPS using a broad range of oils, including synthetic oils, such as silicone oil, and edible food oils, including corn oil, olive oil, and almond oil (*vide infra*). Both food oils and silicone oil are used as models in the work described below. The use of silicone oil enables manipulation of liquid-phase viscosities in fundamental studies and is used widely for the design of conventional SLIPS, permitting comparisons to other liquid-infused materials; SLIPS generated by infusion of food oils into PCL mats are comprised entirely of biodegradable and/or edible components. In the section below, we describe the fabrication and characterization of degradable SLIPS using PCL mats fabricated by electrospinning; characterization of processes based on blow spinning are detailed in subsequent sections.

Fabrication of degradable SLIPS coatings using electrospun PCL mats

Figure 1B shows representative SEM images of porous PCL nanofiber mats fabricated under the conditions used here to design oil-infused surfaces (see Methods for details of electrospinning parameters). These materials are composed of a networks of nanofibers that are randomly aligned and largely devoid of structural defects or features such as beads or

flattened areas (average diameter ~400 nm; see Figure S1 for additional characterization). The thicknesses of these mats can be varied readily by varying electrospinning times; SEM images of cross-sections of mats formed by electrospinning for ~5 min reveal them to have average thicknesses of ~40 μm (Figure 1C). These images also reveal the porosity observed in top-down SEM images shown in Figure 1B to be present throughout the bulk of these materials, consistent with the internal morphologies of PCL nanofiber mats reported in past studies[37,42] and essential for the design of robust liquid-infused surfaces.[14,15]

These electrospun PCL mats can be infused with oils to create coatings that are both slippery and antifouling to several different types of chemically complex liquids. Droplets of silicone oil readily spread across the surfaces of the mats ($\theta \sim 0°$) and infused into the mesh (accompanied by a change in appearance from opaque to transparent). Aqueous droplets placed on 'dry' (non-oil-infused) PCL mats wet the surface of the mat and did not roll or slide off, even when the substrates were tilted at angles as high as 90°. In contrast to this behavior, drops of water slid off of oil-infused coatings unimpeded. The images in Figure 1D provide top-down views of 20 μL droplets of other chemically complex fluids, such as beer, serum, glycerol, human urine, soy sauce, and unfiltered lake water on silicone oil-infused SLIPS tilted at 20°. Droplets of these liquids slid off the surfaces of these substrates (~4 cm) over a period of 5–10 s (see also Video S1). These substrates could be subjected to liquids repeatedly without observable erosion of slippery behavior; additional characterization of other aspects of physical and chemical robustness is described below.

As noted above, these porous PCL meshes can also be infused with other oils, including food oils that are edible and biodegradable. Table 1 provides values of the advancing water contact angles (θ_{adv}), contact angle hysteresis (θ_{hys}), and the sliding angles (θ_s) of water droplets (10 μL) on PCL mats infused with silicone, corn, olive, and almond oils. In each of these cases, aqueous droplets slid at low sliding angles (< 10°) and exhibited $\theta_{hys} < 10°$, demonstrating the robust slippery behaviors of these liquid infused surfaces. In particular, olive oil-infused surfaces exhibited contact angle hysteresis and sliding angles that were significantly lower ($\theta_{hys} < 2°$ and $\theta_s \sim 5°$) than those of the other oils used in this study. These differences in sliding behaviors are consistent with differences in the configurations of the oil-water interfaces formed when aqueous droplets are placed on liquid-infused surfaces.[12,43] For olive oil-infused surfaces, $S_{os(w)} = 0$ (Table S1), suggesting complete wetting and encapsulation of the porous surface underneath the sliding droplet, resulting in extremely low sliding angles (Table 1). For silicone oil-infused surfaces, $-\gamma_{ow}R < S_{os(w)} < 0$ (Table S1), indicative of an emergent porous matrix beneath the droplet (i.e., the tops of the porous surface emerge, to some extent, from the infused silicone oil phase and make contact with the sliding droplets), leading to higher sliding angles and contact angle hysteresis.

Anti-biofouling properties in contact with microorganisms and physiological fluids

We further characterized the ability of these degradable SLIPS-coatings to resist attachment and biofouling (e.g., formation of biofilms) by common fungal and bacterial pathogens. We incubated bare substrates and SLIPS-coated substrates infused with silicone oil with cultures of *Candida albicans* (a fungal pathogen), *Staphylococcus aureus* (a Gram-positive bacterial pathogen), and *Escherichia coli* (a Gram-negative bacterial pathogen) at 37 °C for

24 h (see Methods for details). Staining with FUN-1 or SYTO-9 staining solutions was then used to characterize levels of biofilm by fluorescence microscopy. Figures 2A,C,E reveal the presence of dense biofilms of *C. albicans*, *S. aureus,* and *E. coli* on bare uncoated surfaces. In contrast, inspection of the images of SLIPS-coated substrates in Figures 2B,D,F reveals the absence of fungal and bacterial biofilms on these slippery surfaces. Olive oil-infused PCL meshes also exhibited robust anti-biofouling performance under these conditions (see Figure S2). In combination with these microbiological experiments, we also characterized these surfaces upon exposure to 3T3 cells, a representative mouse fibroblast cell line, for 24 h. Figures 2G,H reveal these SLIPS-coated surfaces to completely prevent adhesion of these mammalian cells under these conditions.

Further investigations showed these degradable SLIPS coatings to repel blood and prevent adhesion of blood components that are involved in thrombosis. Figure 3A shows images of a droplet of pig blood (20 μL) placed on a SLIPS surface infused with silicone oil tilted at 20°. The drop slid over a distance of 4 cm in ~8 s; we observed similar behaviors for olive oil infused-SLIPS. Figure 3B includes a time series showing an uncoated surface (left), and SLIPS-coated surfaces infused with silicone oil (middle) and olive oil (right) after dipping into blood 1, 5, and 10 times. These images reveal both silicone and olive oil infused SLIPS to repel blood after extended and repeated contact (see also Video S2). Finally, Figures 3C–E show SEM images of glass surfaces, glass surfaces coated with nanofibers (no oil), and surfaces coated with SLIPS after exposure to porcine platelet-rich plasma at 37 °C for 1.5 h (see Methods for details). These images reveal dense films of platelets adhered to the bare glass substrate and the nanofiber-coated (no oil) glass substrates. In contrast, SLIPS-coated substrates maintained a stable oil layer, even after exposure of the substrates to a series of dehydration steps in ethanol, and no platelets were observed on the surface (Figure 3E). The SLIPS-coated substrates also exhibited outstanding hemocompatibility, with negligible hemolysis (~1%; similar to that observed for uncoated substrates (~0.9%)) when incubated with human red blood cells. Overall, these results are consistent with the excellent liquid repellency and general anti-fouling behaviors of other non-degradable SLIPS-based materials reported previously.[13,14] These results are significant because they demonstrate that these salient features and useful behaviors of other oil-infused surfaces, often fabricated using complex and multi-step procedures and oils or matrix materials that are not degradable, can be recapitulated by a straightforward fabrication process using common materials that are biodegradable and biocompatible.

Fabrication of degradable SLIPS using solution blow spinning

The overall approach described above for the infusion of oils into PCL mats is also compatible with nanofiber mats fabricated by solution blow spinning (SBS). SBS provides an approach to producing polymer nanofibers that addresses or eliminates several practical limitations associated with electrospinning, including characteristically low nanofiber production rates and the need for electrically conductive targets and high voltages.[39,40] We used SBS to spray PCL solutions of different concentrations (from 5 to 15 wt% in dichloromethane) onto substrates placed ~7.5 cm away from the tip of a hand-held blow spinning nozzle (see illustration in Figure 4A and Methods for additional details). The resulting PCL nanofiber mats exhibited a homogenous nanofiber structure, with average

diameters of ~190 nm and morphologies generally free of structural imperfections (Figure 4B,C; see also Figure S1 for results of additional characterization of nanofiber size distributions). Infusion of oils into these PCL meshes also yielded slippery surfaces. Figure 4D shows the contact angle hysteresis for droplets of water (10 μL) placed on blow-spun mats infused with silicone, olive, corn, and almond oils. These θ_{hys} values were low (< 10°) and generally consistent with those described above on SLIPS fabricated by electrospinning. Figure 4E shows images of a 30 μL water droplet positioned at one end of a tilted slippery surface fabricated by blow spinning; the droplet slid down and across the oil-infused surface at a rate of ~3.3 mm s^{-1}.

Blow spinning is rapid, readily scalable, and permits degradable PCL nanofiber mats to be effectively ‘air brushed’ onto objects of arbitrary shape, size, and composition. Figures 5A–E show images of different model substrates, including a watch glass, a rubber glove, polycarbonate safety glasses, a banana, and a strip of adhesive tape that were coated with uniform and conformal PCL nanofiber-based meshes by blow spinning. These objects were selected for these proof-of-concept studies and for demonstration purposes to represent a variety of natural and synthetic surfaces of different shape, size, transparency, and surface characteristics. Figures 5F–J show images of these coated objects after infusion with oil. These degradable coatings generally became transparent after oil-infusion and exhibited slippery properties (Video S3 shows water droplets sliding on these SLIPS-coated surfaces) that were maintained after physical manipulation and exposure to several different types of complex fluids (including repeated immersion in ketchup (Figures 5K–P, Video S4), exposure to blood (Figures 5Q–V), and manual rubbing or smudging; see Methods). The physically robust nature of the liquid-infused PCL coatings permitted the design of slippery adhesive tape (Figure 5J) that could be affixed to other surfaces to impart slippery and anti-fouling properties (Figure 5W–X; see also Video S5). Overall, these blow spinning strategies for the design of degradable SLIPS offer levels of flexibility and scalability that are more difficult to achieve using electrospinning approaches discussed above and other previously reported SLIPS fabrication procedures.

Controlled release SLIPS: Release of small-molecules from degradable oil-infused PCL mats

These approaches to the design of degradable liquid-infused surfaces also offer means to incorporate or encapsulate molecular cargo by dissolving or dispersing low-molecular weight agents in the PCL solutions used during fabrication. We hypothesized that if it were possible to incorporate other agents into the fibers without substantially altering the surface properties of the resulting PCL nanofibers (thereby permitting the stable infusion of oil), this approach could enable new designs of controlled-release SLIPS and create opportunities for their use in new applied contexts. To explore this approach and demonstrate proof-of-concept, we conducted a series of experiments using PCL fibers loaded with 0.5 wt% of the model small-molecule fluorophore TMR. Figure S3A provides SEM images of nanofiber coatings created by the electrospinning of PCL solutions containing dissolved TMR and shows smooth nanofibers with mean diameters of ~310 nm (see Figure S1 for additional characterization of nanofiber size; Figure S3B shows a fluorescence microscopy image that reveals red filamentous structures consistent with encapsulation of TMR). Infusion of these

loaded PCL mats with silicone oil (ν = 50 cSt) resulted in slippery coatings with sliding angles of ~10°, similar to the PCL-based SLIPS coatings without TMR described above (see Table 1; also see Figure S3C for fluorescence microscopy images of TMR-loaded oil-infused mats).

Figure 6A shows the release profiles of TMR from electrospun mats without infused oil (solid triangles) and mats infused with silicone oil (ν = 50 cst; solid diamonds) upon immersion in PBS at 37 °C. These results reveal PCL mats without infused oil to release TMR rapidly, and with a very large burst release, relative to silicone oil-infused PCL mats, which released TMR slowly and gradually over the 8-day period of this experiment. The burst release behavior of the non-oil-infused mats is consistent with the rapid penetration of water and subsequent desorption and diffusion of water-soluble TMR from the PCL nanofibers[44–46] (we do not interpret this behavior to result from hydrolytic degradation or erosion of PCL upon contact with water, as PCL generally degrades over much more extended periods in physiologically relevant media). These non-oil-infused mats released ~85% of the total amount of loaded TMR from after the first ~8 days; this release profile is generally consistent with those of other small molecules embedded in electrospun PCL-based materials.[44,46,47]

In contrast, silicone oil-infused PCL mats released TMR more slowly (Figure 6A, solid diamonds), a result that we attribute to the ability of the infused oil to prevent rapid infiltration of water upon immersion in PBS (these mats retained oil and remained slippery during the course of these experiments, as revealed by periodic measurement of water droplet sliding times). The sustained release of TMR is likely to be governed, at least in part, by diffusion processes that involve partitioning of TMR from the nanofibers and into the surrounding hosted oil phase, followed by subsequent transport into the surrounding aqueous phase. We note that, for these oil-infused substrates, only ~50% of the TMR that was initially loaded was released over the 8-day course of this experiment. We hypothesized that the release of TMR could be manipulated and tuned by altering the physicochemical properties of the lubricating oil phase. For example, it should be possible to prolong release by increasing viscosity or lowering the temperature of the surrounding environment (and, thereby, lowering the diffusion rate of TMR through the infused oil layer). To test this, we fabricated PCL mats infused with silicone oil having a viscosity 10 times higher (500 cSt; Figure S3D) than that used in the experiments above and performed controlled release experiments at two different temperatures (4 °C and 37 °C). Increasing viscosity slowed release significantly (Figure 6A, solid squares; ~22% of TMR was released over 8 days) compared to mats infused with lower viscosity oil (50 cSt; ~50% released). Release was also substantially slower when these samples were incubated at 4 °C (only 3% was released over the first 8 days (Figure 6A, solid circles); the release of TMR from PCL mats that were not oil-infused was independent of the incubation temperature).

Figure 6B (filled triangles) shows the release profiles of electrospun mats infused with olive oil (ν ~ 40 cSt) in PBS at 37 °C. These olive oil-infused mats also retained their oil and remained slippery during the course of this experiment. However, comparison of these results to those of substrates infused with silicone oil (Figure 6A, solid diamonds) reveals them to release TMR at a faster rate, even though both of the oils used here have

similar viscosities. This result is likely due to increased solubility of TMR in olive oil and accompanying differences in oil/water partition coefficients that could also influence rates at which TMR is transported into the surrounding aqueous phase. When combined, these results demonstrate that the release of incorporated molecules can be manipulated by varying the properties of the infused lubricating fluid. It is likely that the influence of the oil phase on release rates could be exploited to tune release more broadly to generate new and complex release behaviors from these slippery anti-fouling surfaces (for example, by using blends of different oils or by incorporating strategies that provide dynamic control over the properties of the oil).

It is also likely that these strategies could be combined with other approaches to modify the release behaviors of the PCL meshes (for example, altering the fiber structure, levels of drug loading, increasing mesh thickness, or incorporating other drug carrier materials)[47,48] to design SLIPS that can release active agents sequentially, without burst release, or over longer periods. We note that the experiments discussed above were conducted over a period of ~1 week because some of the liquid-infused samples, in particular those infused with silicone oil, exhibited reductions in slippery character (e.g., decreases in droplet sliding times and increases in droplet sliding angles) when incubated in PBS for longer time periods. We attribute these reductions in slippery character to loss of oil from the SLIPS coatings over time, and not physical or chemical changes in the underlying nanofiber matrix (in such cases, re-infusion of additional oil resulted in the recovery of slippery properties, and characterization by SEM did not reveal significant changes in the porous nature of the underlying matrix after a week of incubation in PBS).

The long-term stability of these materials could also be improved, optimized, or tuned, in general, in several other ways, including chemical modification of the PCL (or the use of copolymers of PCL containing more hydrophobic monomers), the incorporation of hydrophobic nano/microparticles during electro/blow spinning, or further manipulation of other fabrication parameters. Several of these strategies have been reported previously to manipulate the surface properties and wetting behaviors of PCL-based mats in other contexts.[49–53] We note, however, that the ability to gradually *drain* lubricating liquid from these materials could also introduce new opportunities to manipulate, and potentially trigger, biodegradation or controlled release behaviors in useful ways. To explore this latter approach, we conducted release experiments similar to those described above in which the surfactant SDS was added to the PBS solutions to trigger a change in the rate at which the infused oil was displaced. The dotted curve in Figure 6A shows the result of this experiment (the red arrow indicates the time at which SDS (10 mg/mL) was introduced into the surrounding media). This result demonstrates that the addition of surface-active agents can significantly enhance the release of TMR from these materials, consistent with an increase in the rate at which oil is removed from these mats (or the rate at which water is able to displace the oil and/or penetrate deeper into the mat; drops of water positioned on coatings after exposure to SDS did not slide and instead completely wet the surface).

In view of the breadth and depth of past studies demonstrating the utility of electro/blow spinning to design PCL nanofibers containing a broad range of other active agents,[41,48] we anticipate that the approaches explored here will also prove useful for the development of

degradable, oil-infused coatings that contain and release other active agents. Apart from the advantages of the inherent anti-fouling properties of these slippery coatings, we note that strategies to manipulate the timing of the displacement of infused oils from these degradable mats could also be useful in other contexts. Finally, we note that the release behaviors described above for oil-infused electrospun PCL mats are also generally applicable to PCL mats fabricated by blow spinning (see Figure S4 for additional discussion). Of note, blow spun PCL mats infused with olive oil maintained robust slippery behavior upon immersion in PBS for at least 45 days.

Summary and Conclusions

We have reported new design principles for the fabrication of SLIPS using building blocks that are biodegradable and biocompatible. These approaches are single-step and straightforward to implement, and useful for coating objects of arbitrary size, composition, and shape. These biocompatible and biodegradable liquid-infused surfaces remain slippery and anti-fouling to a broad range of commercially relevant liquids, viscoelastic materials, mammalian cells, and microorganisms, including several notorious human microbial pathogens. These approaches also permit the incorporation of controlled release behaviors to these inherently anti-fouling materials. Our results show that small molecules can be released from these biodegradable anti-fouling coatings at rates that can be manipulated by the properties of the infused liquid phase or by the rate of displacement of infused oil by a surrounding aqueous phase. Overall, these results provide new design strategies and fabrication techniques that broaden the scope of functions and behaviors exhibited by SLIPS, address emerging challenges related to environmental persistence and biocompatibility, and enable scalable fabrication. These approaches could prove useful for the design of multifunctional and environmentally sustainable antifouling coatings with utility in a broad range of applied contexts.

Supplementary Material

Refer to Web version on PubMed Central for supplementary material.

Acknowledgment.

Financial support was provided by the NSF through a grant to the UW–Madison MRSEC (DMR-1720415) and by grants from the Draper Technology Innovation Fund (Draper-TIF) and the WARF Accelerator Program administered by the UW–Madison Wisconsin Alumni Research Foundation (WARF). Fungal, bacteriological, and mammalian cell assay development was supported in part by the National Institutes of Health (NIH; R35 GM131817 to H.E.B. and R33AI127442 to D.M.L. and S.P.P.). L.J.Q and T.J.P. were partially supported by the UW–Madison NIH CBI Training Program (T32 GM008505). D.H.C. was partially supported by the UW-Madison BTP (T32 GM135066). We acknowledge use of instrumentation supported by the NSF through the UW MRSEC (DMR-1720415). We thank Dr. Visham Appadoo for advice and helpful discussion.

References

1. Marine and Industrial Biofouling, 1 Ed.; Flemming HC; Murthy PS; Venkatesan R; Cooksey KE, Eds.; Springer, 2009.
2. The Role of Biofilms in Device-Related Infections, 1 Ed.; Shirtliff M; Leid JG, Eds.; Springer, 2009.
3. Tuteja A; Choi W; Ma M; Mabry JM; Mazzella SA; Rutledge GC; McKinley GH; Cohen RE Designing Superoleophobic Surfaces. Science 2007, 318, 1618. [PubMed: 18063796]

4. Banerjee I; Pangule RC; Kane RS Antifouling Coatings: Recent Developments in the Design of Surfaces That Prevent Fouling by Proteins, Bacteria, and Marine Organisms. Adv. Mater 2011, 23, 690–718. [PubMed: 20886559]
5. Yao X; Song Y; Jiang L Applications of Bio-Inspired Special Wettable Surfaces. Adv. Mater 2011, 23, 719–734. [PubMed: 21287632]
6. Liu K; Jiang L Bio-Inspired Self-Cleaning Surfaces. Annual Review of Materials Research 2012, 42, 231–263.
7. Campoccia D; Montanaro L; Arciola CR A Review of the Biomaterials Technologies for Infection-Resistant Surfaces. Biomaterials 2013, 34, 8533–8554. [PubMed: 23953781]
8. Chu Z; Seeger S Superamphiphobic Surfaces. Chem. Soc. Rev 2014, 43, 2784–2798. [PubMed: 24480921]
9. Zander ZK; Becker ML Antimicrobial and Antifouling Strategies for Polymeric Medical Devices. ACS Macro Lett 2018, 7, 16–25. [PubMed: 35610930]
10. Wong TS; Kang SH; Tang SKY; Smythe EJ; Hatton BD; Grinthal A; Aizenberg J Bioinspired Self-Repairing Slippery Surfaces with Pressure-Stable Omniphobicity. Nature 2011, 477, 443–447. [PubMed: 21938066]
11. Lafuma A; Quéré D Slippery Pre-Suffused Surfaces. EPL (Europhysics Letters) 2011, 96, 56001.
12. Smith JD; Dhiman R; Anand S; Reza-Garduno E; Cohen RE; McKinley GH; Varanasi KK Droplet Mobility on Lubricant-Impregnated Surfaces. Soft Matter 2013, 9, 1772–1780.
13. Sotiri I; Overton JC; Waterhouse A; Howell C Immobilized Liquid Layers: A New Approach to Anti-Adhesion Surfaces for Medical Applications. Exp. Biol. Med 2016, 241, 909–918.
14. Solomon BR; Subramanyam SB; Farnham TA; Khalil KS; Anand S; Varanasi KK, Chapter 10 Lubricant-Impregnated Surfaces. In Non-Wettable Surfaces: Theory, Preparation and Applications, The Royal Society of Chemistry: 2017; pp 285–318.
15. Villegas M; Zhang Y; Abu Jarad N; Soleymani L; Didar TF Liquid-Infused Surfaces: A Review of Theory, Design, and Applications. ACS Nano 2019, 13, 8517–8536. [PubMed: 31373794]
16. Regan DP; Howell C Droplet Manipulation with Bioinspired Liquid-Infused Surfaces: A Review of Recent Progress and Potential for Integrated Detection. Curr. Opin. Colloid Interface Sci 2019, 39, 137–147.
17. Yao X; Hu Y; Grinthal A; Wong T-S; Mahadevan L; Aizenberg J Adaptive Fluid-Infused Porous Films with Tunable Transparency and Wettability. Nat. Mater 2013, 12, 529–534. [PubMed: 23563739]
18. Wang W; Timonen JVI; Carlson A; Drotlef D-M; Zhang CT; Kolle S; Grinthal A; Wong T-S; Hatton B; Kang SH; Kennedy S; Chi J; Blough RT; Sitti M; Mahadevan L; Aizenberg J Multifunctional Ferrofluid-Infused Surfaces with Reconfigurable Multiscale Topography. Nature 2018, 559, 77–82. [PubMed: 29942075]
19. Epstein AK; Wong T-S; Belisle RA; Boggs EM; Aizenberg J Liquid-Infused Structured Surfaces with Exceptional Anti-Biofouling Performance. Proc. Natl. Acad. Sci. U. S. A 2012, 109, 13182–13187. [PubMed: 22847405]
20. Xiao L; Li J; Mieszkin S; Di Fino A; Clare AS; Callow ME; Callow JA; Grunze M; Rosenhahn A; Levkin PA Slippery Liquid-Infused Porous Surfaces Showing Marine Antibiofouling Properties. ACS Appl. Mater. Interfaces 2013, 5, 10074–10080. [PubMed: 24067279]
21. Leslie DC; Waterhouse A; Berthet JB; Valentin TM; Watters AL; Jain A; Kim P; Hatton BD; Nedder A; Donovan K; Super EH; Howell C; Johnson CP; Vu TL; Bolgen DE; Rifai S; Hansen AR; Aizenberg M; Super M; Aizenberg J; Ingber DE A Bioinspired Omniphobic Surface Coating on Medical Devices Prevents Thrombosis and Biofouling. Nat. Biotechnol 2014, 32, 1134–1140. [PubMed: 25306244]
22. Manabe K; Kyung K-H; Shiratori S Biocompatible Slippery Fluid-Infused Films Composed of Chitosan and Alginate Via Layer-by-Layer Self-Assembly and Their Antithrombogenicity. ACS Appl. Mater. Interfaces 2015, 7, 4763–4771. [PubMed: 25646977]
23. Kratochvil MJ; Welsh MA; Manna U; Ortiz BJ; Blackwell HE; Lynn DM Slippery Liquid-Infused Porous Surfaces That Prevent Bacterial Surface Fouling and Inhibit Virulence Phenotypes in Surrounding Planktonic Cells. ACS Infect. Dis 2016, 2, 509–517. [PubMed: 27626103]

24. Yuan S; Li Z; Song L; Shi H; Luan S; Yin J Liquid-Infused Poly(Styrene-b-Isobutylene-b-Styrene) Microfiber Coating Prevents Bacterial Attachment and Thrombosis. ACS Appl. Mater. Interfaces 2016, 8, 21214–21220. [PubMed: 27482919]
25. Manna U; Raman N; Welsh MA; Zayas-Gonzalez YM; Blackwell HE; Palecek SP; Lynn DM Slippery Liquid-Infused Porous Surfaces That Prevent Microbial Surface Fouling and Kill Non-Adherent Pathogens in Surrounding Media: A Controlled Release Approach. Adv. Funct. Mater 2016, 26, 3599–3611. [PubMed: 28713229]
26. Solomon BR; Khalil KS; Varanasi KK Drag Reduction Using Lubricant-Impregnated Surfaces in Viscous Laminar Flow. Langmuir 2014, 30, 10970–10976. [PubMed: 25144426]
27. Rosenberg BJ; Van Buren T; Fu MK; Smits AJ Turbulent Drag Reduction over Air- and Liquid-Impregnated Surfaces. Phys. Fluids 2016, 28, 015103.
28. Kim P; Wong T-S; Alvarenga J; Kreder MJ; Adorno-Martinez WE; Aizenberg J Liquid-Infused Nanostructured Surfaces with Extreme Anti-Ice and Anti-Frost Performance. ACS Nano 2012, 6, 6569–6577. [PubMed: 22680067]
29. Subramanyam SB; Rykaczewski K; Varanasi KK Ice Adhesion on Lubricant-Impregnated Textured Surfaces. Langmuir 2013, 29, 13414–13418. [PubMed: 24070257]
30. Agarwal H; Nyffeler KE; Blackwell HE; Lynn DM Fabrication of Slippery Liquid-Infused Coatings in Flexible Narrow-Bore Tubing. ACS Appl. Mater. Interfaces 2021, 13, 55621–55632. [PubMed: 34775755]
31. Agarwal H; Breining WM; Lynn DM Continuous Fabrication of Slippery Liquid-Infused Coatings on Rolls of Flexible Materials. ACS Appl. Polym. Mater 2022, 4, 787–795.
32. Agarwal H; Breining WM; Sánchez-Velázquez G; Lynn DM Reactive Multilayers and Coatings Fabricated by Spray Assembly: Influence of Polymer Structure and Process Parameters on Multiscale Structure and Interfacial Properties. Chem. Mater 2022, 34, 1245–1258.
33. Kratochvil MJ; Yang T; Blackwell HE; Lynn DM Nonwoven Polymer Nanofiber Coatings That Inhibit Quorum Sensing in Staphylococcus aureus: Toward New Nonbactericidal Approaches to Infection Control. ACS Infect. Dis 2017, 3, 271–280. [PubMed: 28118541]
34. Novick RP; Ross HF; Projan SJ; Kornblum J; Kreiswirth B; Moghazeh S Synthesis of Staphylococcal Virulence Factors Is Controlled by a Regulatory RNA Molecule. The EMBO journal 1993, 12, 3967–3975. [PubMed: 7691599]
35. Raguse TL; Porter EA; Weisblum B; Gellman SH Structure–Activity Studies of 14-Helical Antimicrobial β-Peptides: Probing the Relationship between Conformational Stability and Antimicrobial Potency. J. Am. Chem. Soc 2002, 124, 12774–12785. [PubMed: 12392424]
36. Porter EA; Weisblum B; Gellman SH Use of Parallel Synthesis to Probe Structure–Activity Relationships among 12-Helical β-Peptides: Evidence of a Limit on Antimicrobial Activity. J. Am. Chem. Soc 2005, 127, 11516–11529. [PubMed: 16089482]
37. Pham QP; Sharma U; Mikos AG Electrospinning of Polymeric Nanofibers for Tissue Engineering Applications: A Review. Tissue Eng 2006, 12, 1197–1211. [PubMed: 16771634]
38. Teo WE; Ramakrishna S A Review on Electrospinning Design and Nanofibre Assemblies. Nanotechnology 2006, 17, R89–R106. [PubMed: 19661572]
39. Daristotle JL; Behrens AM; Sandler AD; Kofinas P A Review of the Fundamental Principles and Applications of Solution Blow Spinning. ACS Appl. Mater. Interfaces 2016, 8, 34951–34963. [PubMed: 27966857]
40. Gao Y; Zhang J; Su Y; Wang H; Wang X-X; Huang L-P; Yu M; Ramakrishna S; Long Y-Z Recent Progress and Challenges in Solution Blow Spinning. Materials Horizons 2021, 8, 426–446. [PubMed: 34821263]
41. Woodruff MA; Hutmacher DW The Return of a Forgotten Polymer—Polycaprolactone in the 21st Century. Prog. Polym. Sci 2010, 35, 1217–1256.
42. Cipitria A; Skelton A; Dargaville TR; Dalton PD; Hutmacher DW Design, Fabrication and Characterization of PCL Electrospun Scaffolds—A Review. J. Mater. Chem 2011, 21, 9419–9453.
43. Preston DJ; Song Y; Lu Z; Antao DS; Wang EN Design of Lubricant Infused Surfaces. ACS Appl. Mater. Interfaces 2017, 9, 42383–42392. [PubMed: 29121462]
44. Srikar R; Yarin AL; Megaridis CM; Bazilevsky AV; Kelley E Desorption-Limited Mechanism of Release from Polymer Nanofibers. Langmuir 2008, 24, 965–974. [PubMed: 18076196]

45. Yohe ST; Colson YL; Grinstaff MW Superhydrophobic Materials for Tunable Drug Release: Using Displacement of Air to Control Delivery Rates. J. Am. Chem. Soc 2012, 134, 2016–2019. [PubMed: 22279966]

46. Carson D; Jiang Y; Woodrow KA Tunable Release of Multiclass Anti-HIV Drugs That Are Water-Soluble and Loaded at High Drug Content in Polyester Blended Electrospun Fibers. Pharm. Res 2016, 33, 125–136. [PubMed: 26286184]

47. Chou S-F; Carson D; Woodrow KA Current Strategies for Sustaining Drug Release from Electrospun Nanofibers. J. Controlled Release 2015, 220, 584–591.

48. Torres-Martinez EJ; Cornejo Bravo JM; Serrano Medina A; Pérez González GL; Villarreal Gómez LJ A Summary of Electrospun Nanofibers as Drug Delivery System: Drugs Loaded and Biopolymers Used as Matrices. Curr. Drug Del 2018, 15, 1360–1374.

49. Ma M; Mao Y; Gupta M; Gleason KK; Rutledge GC Superhydrophobic Fabrics Produced by Electrospinning and Chemical Vapor Deposition. Macromolecules 2005, 38, 9742–9748.

50. Han D; Steckl AJ Superhydrophobic and Oleophobic Fibers by Coaxial Electrospinning. Langmuir 2009, 25, 9454–9462. [PubMed: 19374456]

51. Kaplan JA; Lei H; Liu R; Padera R; Colson YL; Grinstaff MW Imparting Superhydrophobicity to Biodegradable Poly(Lactide-co-Glycolide) Electrospun Meshes. Biomacromolecules 2014, 15, 2548–2554. [PubMed: 24901038]

52. C. R R; Sundaran SP; A J; Athiyanathil S Fabrication of Superhydrophobic Polycaprolactone/Beeswax Electrospun Membranes for High-Efficiency Oil/Water Separation. RSC Advances 2017, 7, 2092–2102.

53. Zhang G; Wang P; Zhang X; Xiang C; Li L The Preparation of PCL/MSO/SiO_2 Hierarchical Superhydrophobic Mats for Oil-Water Separation by One-Step Method. Eur. Polym. J 2019, 116, 386–393.

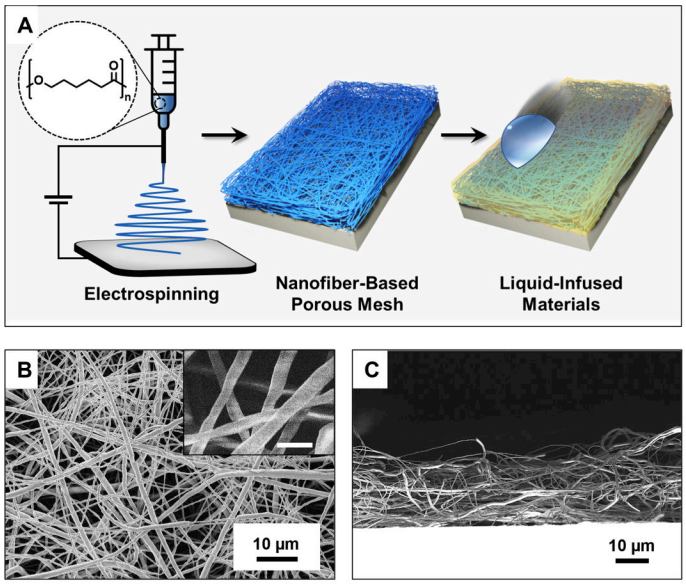

Table 1: Impact of Infused Oil on Sliding Behavior

Infused-Liquid	Θ_{Adv} (°)	Θ_{hys} (°)	θ_s(°)
Silicone	93 ± 3	6 ± 1	9 ± 2
Corn	65 ± 5	8 ± 1	10 ± 2
Olive	82 ± 2	< 2	5 ± 2
Almond	82 ± 3	5 ± 1	10 ± 3

Figure 1.

A) Schematic showing the electrospinning-based approach used to fabricate degradable nanofiber-based SLIPS. The structure of PCL is also shown. B,C) Top-down (B) and cross-sectional (C) SEM images of PCL-nanofiber meshes fabricated by electrospinning; scale bar of inset in B is 500 nm. D) Droplets of water and other complex fluids sliding down strips of Al foil coated with SLIPS; droplets were 20 μL and tilt angle was 20°; the water contained a pink dye. Table 1 shows values of θ_{adv}, θ_{hys}, and θ_s for 10 μL water droplets on porous PCL meshes infused with silicone, corn, olive, and almond oils.

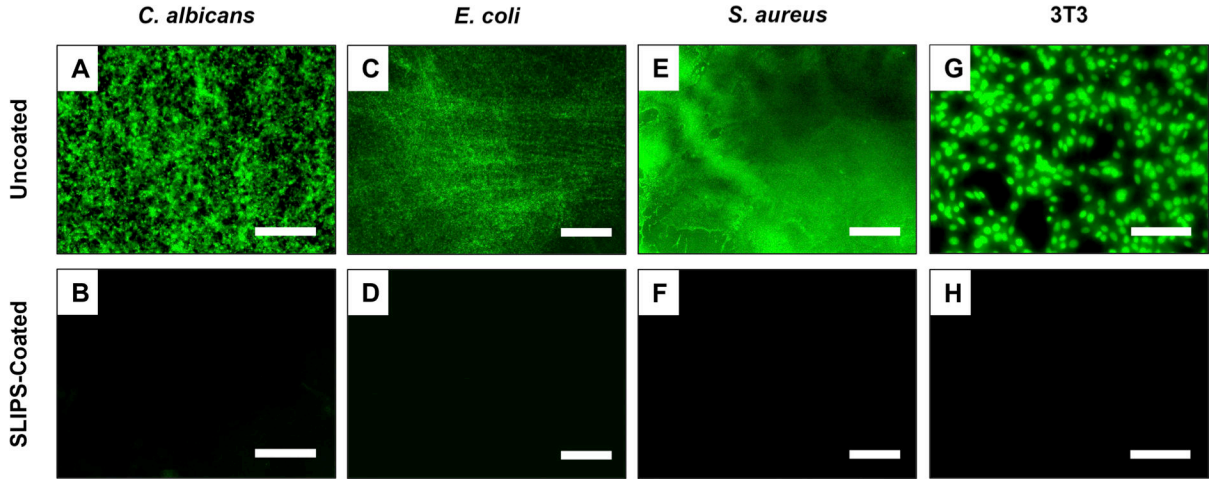

Figure 2.

A–F) Images of uncoated and SLIPS-coated surfaces exposed to cultures of *C. albicans* (A,B) *E. coli* (C,D), and *S. aureus* (E,F) for 24 h; *C. albicans* was stained with FUN-1 fluorescent dye and *E. coli* and *S. aureus* were stained using SYTO-9 before imaging by fluorescence microscopy. G,H) Images of uncoated and SLIPS-coated surfaces exposed to 3T3 cells for 48 h; samples were stained with SYTO-9 before imaging by fluorescence microscopy. Scale bars are 200 μm in (A,B), 400 μm in (C-F), and 100 μm in (G-H).

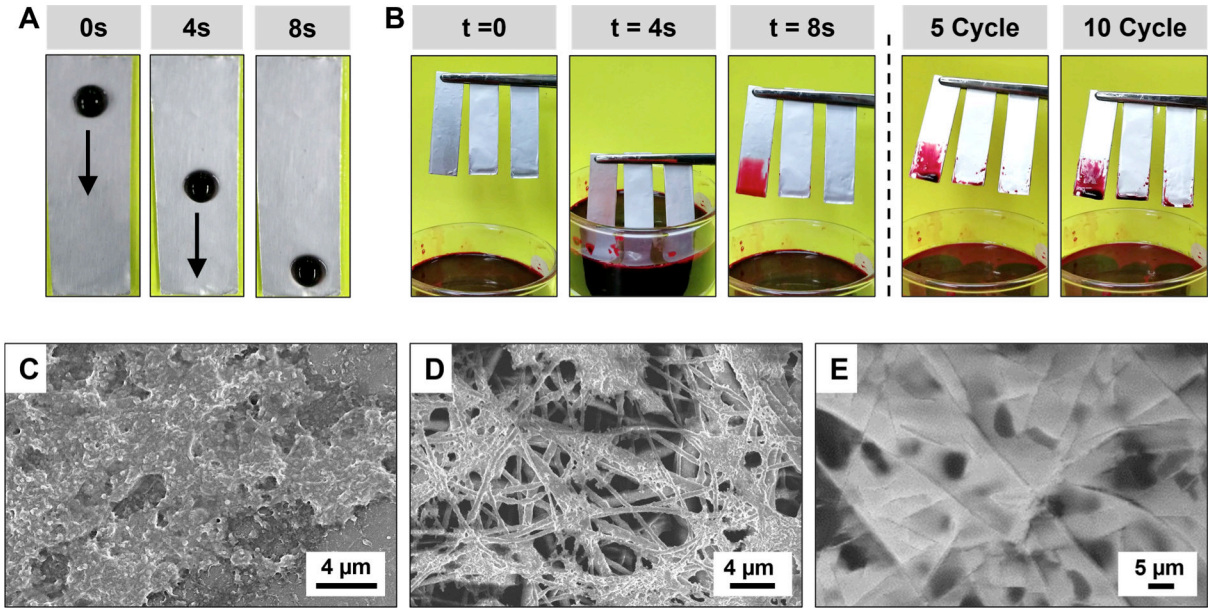

Figure 3.

A) Pictures showing a droplet of blood (20 μL; tilt angle ≈ 20°) on a SLIPS-coated surface (~ 4 × 1cm) infused with silicone oil. B) Images of PCL nanofiber-coated substrates (non-infused (left), infused with silicone oil (middle), and infused with olive oil (right)) before and after dipping in blood multiple times; time-series images are shown for the first cycle only. C-E) SEM images of platelet adhesion on (C) bare glass, (D) PCL nanofiber-coated glass with no infused oil, and (E) SLIPS-coated substrates.

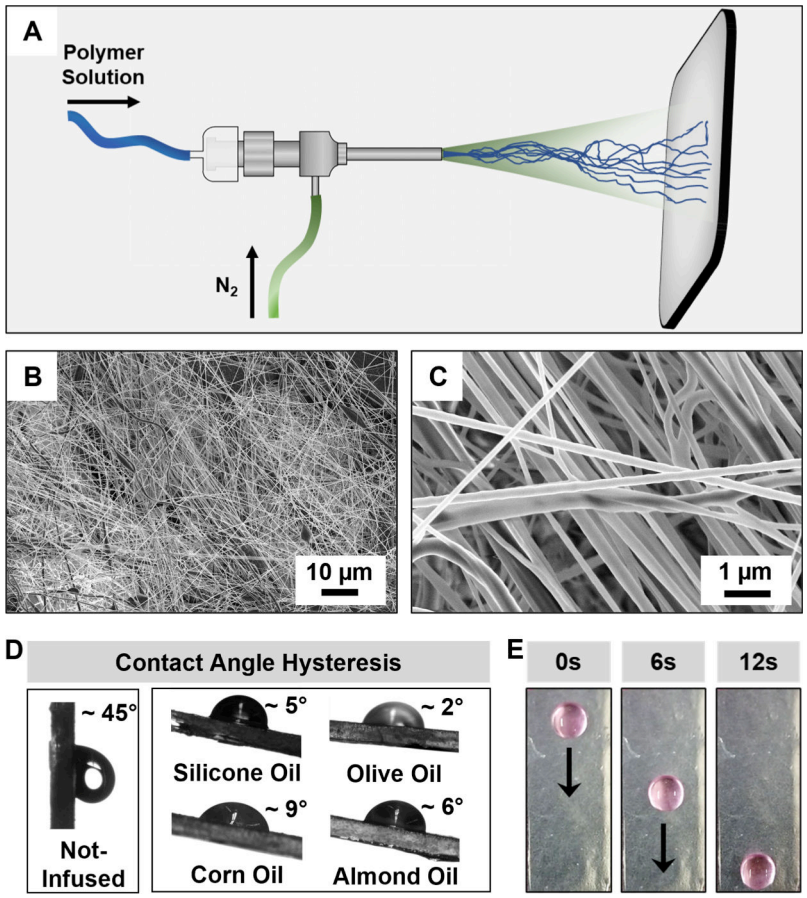

Figure 4.

A) Illustration showing solution blow spinning approaches to the fabrication of PCL nanofiber-based mats. B,C) SEM images of PCL mats fabricated by blow spinning a 5 wt% solution of PCL in dichloromethane; see Figure S1 for additional characterization. D) Images showing contact angle hysteresis (θ_{hys}) of a mat that was not infused with oil (left) and mats that were infused with silicone, olive, corn, and almond oil (right). The tilt angles (θ_{tilt}) shown are 90° for the non-infused sample, 10° for the silicone, corn, and almond oil-infused substrates, and 5° for the olive oil-infused substrate. E) Pictures of a droplet of water containing TMR (30 μL; tilt angle ≈ 20°) sliding across a 4 cm long silicone oil-infused coating fabricated by blow spinning.

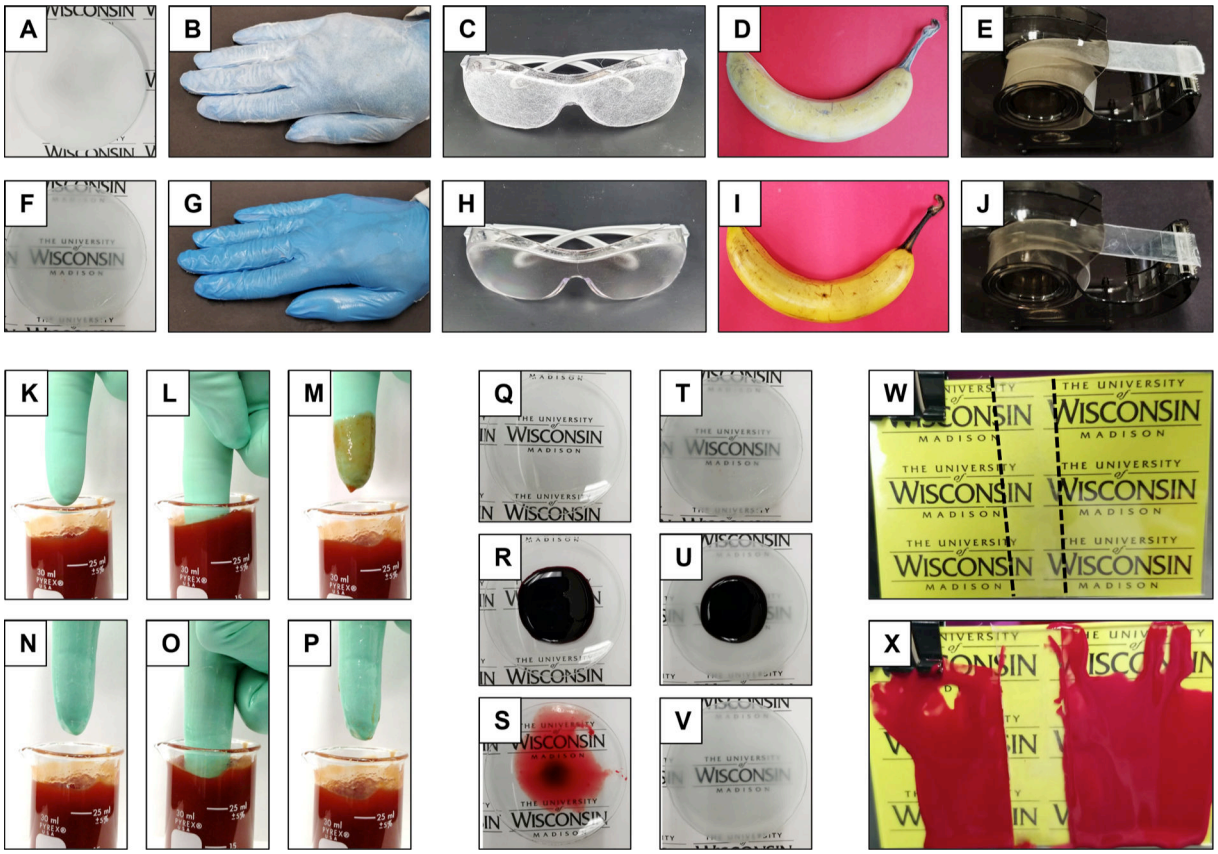

Figure 5.

A–J) Images of objects coated with PCL nanofiber mats fabricated using blow spinning: (A) watch glass, (B) rubber nitrile glove, (C) polycarbonate safety glasses, (D) banana, and (E) a strip of double-sided adhesive tape. Panels (F–J) show the same objects after infusion with silicone oil. (K–P) Images of an uncoated gloved finger (K–M) and a SLIPS-coated gloved finger (N–P) upon immersion and removal from a sample of ketchup. Q–V) Pictures of a bare (uncoated) watch glass (Q–S) and a SLIPS-coated watch glass (T–V) upon exposure to and draining of blood. W) Picture of SLIPS-coated adhesive tape stuck on the surface of a bare glass plate; the edges of the SLIPS-coated tape are marked with dashed lines to guide the eye. The image in (X) shows the same surface in (W) after splashing the entire surface with red water-based paint; the area of the substrate coated with the slippery tape remained clean. See also Videos S3–S5. The logo shown in panels A, F, and Q-X is used with permission granted by the University of Wisconsin–Madison.

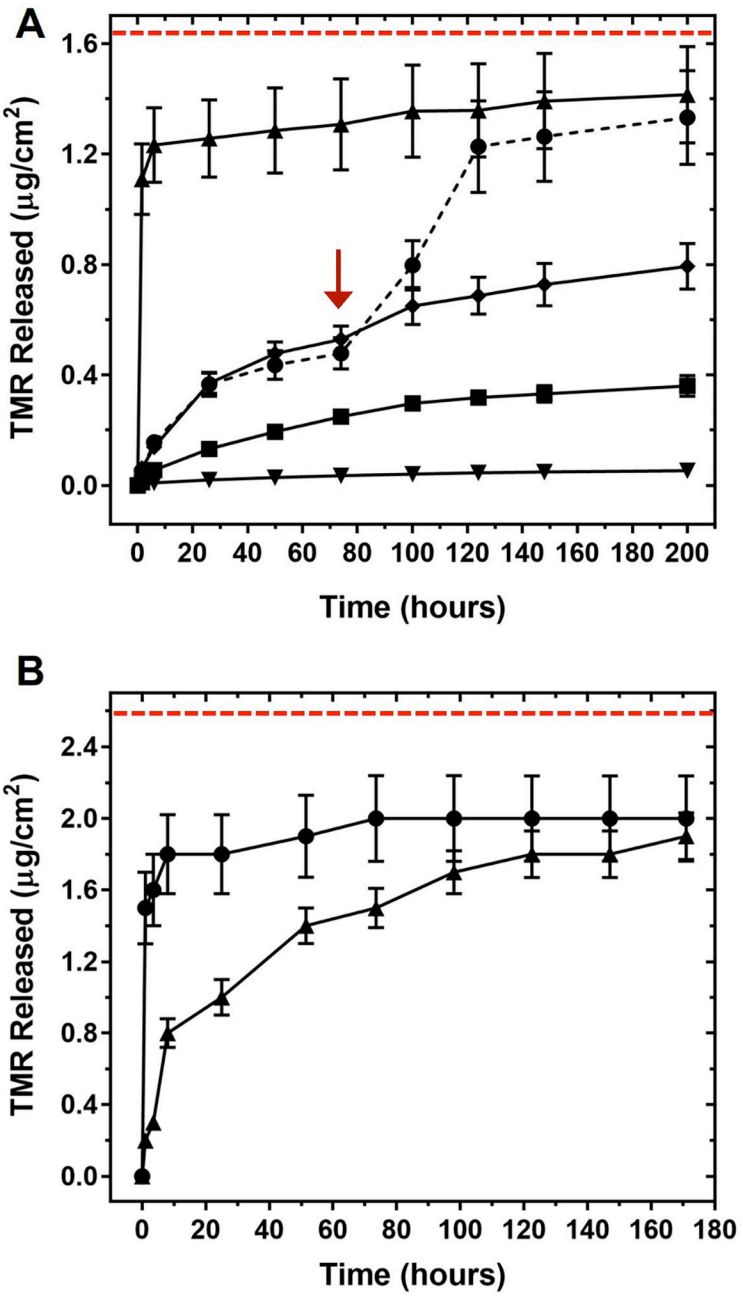

Figure 6.

A) Plot showing release of TMR from TMR-loaded PCL mats (loading amount = 1.64 ± 0.16 μg cm^{-2}, marked by dotted red line) after immersion in PBS at 37 °C. Symbols correspond to coatings that do not contain infused oil (▲) and coatings that are infused with silicone oil (ν= 50 cSt (♦) or 500 cSt (■)). The symbol (▼) corresponds to the release profile of mats infused with silicone oil (ν = 500 cSt) incubated at 4 °C. During some experiments using mats infused with silicone oil (50 cSt), 10 mg/mL SDS was added at a time indicated by the red arrow; the results of these experiments are indicated with closed circles (●) and a dotted line. B) Plot showing release of TMR from TMR-loaded PCL mats (loading amount = 2.58 ± 0.5 μg cm^{-2}, marked by dotted red line) infused with olive oil

(▲) and not infused with oil (●) upon incubation in PBS at 37 °C. The error bars denote standard deviations and are in some cases smaller than the symbols.